


Raman spectroscopy and its reliability in the study of bone quality and composition.


2/11/2013

The reliability of Raman spectroscopy in the study of bone composition and quality is reviewed. The equipment selection used by several authors is compared, and conclusions drawn about the advantages and disadvantages of each. Orientation effects and spectral band assignments are questioned.

CONTENTS

Introduction	2
1 An introduction to the Raman Effect in molecular systems	3
2 Raman spectroscopy: Equipment and its advantages in the study of bone composition.....	4
2.1 Dispersive Raman spectrometers	5
2.2 Fourier transform Raman spectrometers.....	6
2.3 The advantages of Raman spectroscopy in the study of bone composition.....	7
3 Bone composition and the use of Raman spectroscopy to assess bone quality	8
3.1 Bone composition	8
3.2 Orientation effects and the assessment of bone quality.....	11
4 Equipment selection.....	14
4.1 Laser selection	14
5 Band assignments of Hydroxyapatite Raman spectra.....	18
5.1 Tracing original band assignments	19
5.2 The reliability of original band assignments.....	22
Discussion.....	24
References.....	25

Introduction

The use of Raman spectroscopy as a tool for cell analysis in Biology has seen a dramatic increase over the last few years. In particular the spectrum of bone is widely investigated. There is extensive literature detailing the use of spectroscopy to study bone due to its ability to analyse mineral content, mineral crystallinity, acid phosphate and carbonate content non-destructively using small sample volumes (4).

Raman spectroscopy possesses many advantages over other imaging techniques when applied to the study of bone composition; it gives excellent spatial resolution (0.6 - 1 μ m), rapid data collection, and is applicable to the analysis of live tissue since it does not damage cells (5). This enables the analysis of biologically important localities, which is impossible with other imaging techniques due to spatial resolution limitations. Small local variations in the bone can be found using multivariate statistics, and information can be obtained from the mineral and organic matrix components of bone simultaneously (6).

The selection of equipment differs amongst authors. Most often in Biology a micro-spectrometer is used (7-10). However, a micro-spectrometer is not ideal for bone imaging as it cannot adequately describe the chemical nature of bone due to its heterogeneous nature (5). The selection of a Laser source is also widely mentioned in literature (11-14) where it is implied that the selection of an excitation source is crucial and can affect the reliability of results. A detailed investigation surrounding laser excitation sources used to generate Raman spectra of Hydroxyapatite contradicts this, and reveals that the spectra is largely unaffected by laser wavelength or power.

Bone is a composite consisting of mineral, an organic matrix, cells, and water (15). Hydroxyapatite is the mineral component of bone and is composed of Phosphate and Calcium. It forms approximately 65% of adult bone (16) and is a major component of human tooth enamel and dentin. Hydroxyapatite is bioactive and can be used to integrate into bone structures within the human body. It is therefore of great interest to the fields of tissue

engineering, biology, and medicine and the crystal structure of Hydroxyapatite is frequently studied.

The major band assignments of Hydroxyapatite are often referred to as having been previously assigned, with little or no evidence of investigation into their origin. A reference trail from recently published papers in Biology and Tissue Engineering can be traced to the original band assignments made tentatively in 1971 (2). The threat to the field of Tissue Engineering is huge if these band assignments, which are so often relied upon, are incorrect. There is therefore a pressing opportunity for the original band assignments to be reviewed.

1 An introduction to the Raman Effect in molecular systems

Raman spectroscopy is a vibrational technique used to evaluate scattered light from a biological molecule or ion (17). As monochromatic light of frequency f_1 is incident on a molecule, a polarization is induced by the oscillating electric field of the incoming light. Most of the light passes through the molecule without change, however a small number of photons exchange energy with vibrations in the molecule and are scattered from it (18). If the frequency of this radiation is analysed it can be observed at f_1 , with a pair of frequencies at $f_1 \pm f_M$ (19). In molecular systems, the frequencies at f_m lie principally in the range of transitions between rotational, vibrational, and electronic levels. The intensity and polarization of the scattered radiation depends on the direction of observation (19, 20).

Scattering with no change of frequency f_1 is termed Rayleigh scattering, and occurs when the incident laser light causes the position of the electron cloud (which forms a chemical bond) to oscillate (21). The oscillation of the electron cloud results in the emission of photons with the same frequency and energy as the incident light. Scattering represented by a change in frequency $f_1 \pm f_M$ is labelled Raman scattering. This occurs when the system makes a transition between energy states and the vibrational energy of the molecule changes. When the spectrum of the scattered radiation is displayed, new frequencies are termed Raman bands and form a Raman spectrum when observed together (22).

Raman frequencies of position $f_1 - f_M$ are Stokes bands and represent a system in the ground vibrational state E_1 absorbing energy and being promoted to a higher energy state E_2 . The system must then gain the necessary energy $\Delta E = E_2 - E_1$ from the incident radiation. The energy gain ΔE can also be represented in terms of the wavenumber associated with the two energy levels, $\Delta E = hc \underline{\omega}_M$ (20, 21). Due to thermal energy some systems can be present in the higher energy state, and therefore scattering from these states to the ground state can occur. This results in emitted energy $E_2 - E_1 = hc \underline{\omega}_M$ (23). This is termed anti-Stokes scattering and is represented in the spectra by the $f_1 + f_M$ Raman bands (19, 20).

The Raman Effect is inherently weak, with approximately one in every $10^6 - 10^8$ scattered photons being Raman scattered (12). The intensity of scattering is directly related to the number of molecules being illuminated (21), the intensity of the incident light, and to $(\nu_0 - \nu)^4$ (where ν_0 is the laser excitation frequency in Hertz, and ν is the molecular vibrational frequency (12)). It is therefore immediately obvious that to improve Raman sensitivity a laser of the highest frequency available should be used. However, high frequency radiation is also high energy and therefore carries a greater risk of sample degradation. Resonance with electronic transitions may also occur, which could cause absorption and alter the spectra (24).

2 Raman spectroscopy: Equipment and its advantages in the study of bone composition

Raman spectroscopy utilizes the Raman Effect in order to obtain the structural and chemical information of a sample. Spectroscopy is an extremely sensitive technique, therefore careful equipment selection is important in order to obtain an accurate spectrum which can be used to successfully study bone composition.

It should also be noted that Infrared and Raman spectroscopy are complementary of each other. In certain molecules which contain a chemical compound with a centre of symmetry, some normal vibrations will be Raman active and others will be Infrared active. Strong Infrared bands are related to polar functional groups and are usually weak in the Raman

spectrum where non polar functions are strongest (12). Therefore in order to record the complete vibrational spectrum of a molecule, both techniques must be employed.

There are two main types of spectrometer design; Fourier transform and dispersive. Both designs begin with a monochromatic laser, which is focussed on the sample using conventional refractive optics (25) [Laser selection is further discussed in chapter 4]. Photons are scattered from the sample as described by the Raman Effect, and the vibrational frequency (ν_m) is measured as a shift from the frequency of the incident laser beam (26).

2.1 Dispersive Raman spectrometers

In dispersive spectrometers, Raman scattered light is focussed onto a diffraction grating which splits the light into its constituent wavelengths. Diffraction gratings consist of a large number of parallel, closely spaced slits. By using a large number of slits as opposed to one or two, the intensity maximum produced is very sharp and narrow which provides the excellent spatial resolution essential for the Raman spectroscopy of bone (27). If spatial resolution is too low then it may become difficult to distinguish between two compounds. On the other hand, if spatial resolution is too high, the spectrum may become unnecessarily noisy without providing any additional useful information (23).

The constituent wavelengths are then directed onto a silicon charge coupled detector (CCD) which produces the readable signal. CCD detectors are a series of individual pixels arranged into a 2D array. When photons are incident on a pixel, it produces electron-hole pairs in proportion to the intensity of the incident light (28). The charge stored in each pixel is subject to a gating voltage which is applied to the electrodes. This enables the charge to be transferred across the array. At the edge of the array, the charge is transferred to an amplifier which converts the charge signal into a voltage. The analogue voltage is processed and converted into a digital signal for computer processing in order to display the spectrum (28).

Cooled CCDs are often applied to dispersive spectrometers; they are multichannel devices and boast exceptional sensitivity and an improved signal-to-noise ratio when compared to non-cooled CCDs. They have a very low intrinsic noise and data acquisition is equally as fast (29).

2.2 Fourier transform Raman spectrometers

Fourier-transform (hereafter FT) Raman spectroscopy is an extremely fast growing analytical technique in chemical and live cell analysis. First suggested by Chantry *et al* (30) in 1964, FT has been developed as an extension of conventional Raman techniques and is widely applied to the study of bone. The equipment used differs slightly from the equipment used in dispersive spectrometers. Firstly, the laser excitation source is exclusively in the near infrared (NIR) range (26) whereas lasers employed by dispersive spectrometers are typically in the visible or ultraviolet range.

Secondly, a FT spectrometer is built around a highly efficient interferometer which is used instead of a diffraction grating to analyse scattered light (31). A filter is used to remove the Rayleigh band which can mask the Raman bands and render them unobservable due to the noise redistribution characteristic of FT Raman (32). The interferometer enables the measurement of light intensity simultaneously at many wavelengths. The spectrum can then be converted to a conventional spectrum by an integrated computer program which applies a Fourier transform.

The advantages of using FT- spectrometers are extensive in the study of bone composition. The main advantage is that it almost entirely eliminates fluorescence. Fluorescence was previously responsible for huge difficulties in obtaining a spectrum from bone in early Raman spectroscopy (3, 33), as the proteins in bone fluoresce and produce a background signal several orders of magnitude higher than the Raman spectra (34). Bone was often deproteinated in an attempt to combat fluorescence (35, 36), which isolates the mineral component of bone but may result in structural or chemical damage which affects the reliability of the results (37).

The multiplex (or Fellgett) advantage of FT-Raman allows wavelengths of light to be detected simultaneously. The throughput (or Jacquinot) advantage means that the energy throughput in an interferometer can be higher than in a dispersive instrument, where it is restricted by the grating (38). The two advantages combined provide FT spectrometers with a

similar signal-to-noise ratio to dispersive instruments, but with a much shorter exposure time (39). This can be advantageous in the study of bone composition as it minimizes the risk of sample degradation.

A potential pitfall of FT-Raman in the study of bone composition is the thermal background emission caused by aqueous solutions. Overtone absorptions in the O-H stretch mode result in the sample absorbing a proportion of incident laser intensity (38). This can cause the temperature of the sample to rise and may produce background emission in the spectral region of interest.

The advantages of FT-Raman spectroscopy outweigh its disadvantages and, providing the Rayleigh line is sufficiently filtered, it can be an extremely beneficial technique in the study of bone composition. However, newcomers to the technique and those who are unfamiliar with the Physics of FT-Raman spectroscopy may experience erroneous results since additional bands are observed which may be confused with the spectrum of the sample (38).

2.3 The advantages of Raman spectroscopy in the study of bone composition

Traditional imaging techniques used for the compositional and structural analysis of bone include; electron microscopy, x-ray diffraction, light microscopy, nuclear magnetic resonance, and chemical analysis (40). These techniques require extensive sample preparation which may alter the composition of the bone, meaning that any conclusions drawn may be unreliable. The advantages of Raman spectroscopy outweigh all of the previous techniques when applied to the study of bone.

Firstly, Raman spectroscopy requires minimal sample preparation and real bone samples can be studied without altering their composition or structure (41). This is extremely important as it improves the accuracy of the obtained spectrum, and any conclusions associated with it. The exposure itself is non-destructive which enables numerous spectra to be recorded from the same sample for analysis (42). Live cell cultures can be imaged, providing invaluable information about their chemical and structural composition whilst allowing the sample to continue to grow.

Secondly, the diffraction limited spatial resolution of Raman spectroscopy is superior to any other technique (approximately 1 μ m). This excellent spatial resolution provides ultra-structural level information, which enables the observation of microscopic phenomena and detailed investigation using small sample volumes. Simultaneous information from the mineral and organic matrix components of bone can be obtained (6) which provides a complete picture of the composition of bone in the area studied.

Since Raman spectra experience little interference from water vibrations, biological samples do not need to be dehydrated. It also enables bone to be imaged in aqueous solutions such as bioreactors, which closely resemble the human body (34). The wavenumber values displayed in the spectrum are extremely accurate and are used to investigate molecular conformations, functional groups and bonding types (42). Spatially relevant information can be obtained when Raman spectra are collected over a two dimensional area (6).

3 Bone composition and the use of Raman spectroscopy to assess bone quality

In recent literature, Raman spectroscopy is extensively used to study the structure and composition of bone (43-48). The degree of mineralization of the collagen matrix, carbonate substitution, and mineral crystallinity are often used to determine bone quality and hence identify diseased bone with ailments such as osteoporosis and osteogenesis imperfecta (49). The degree of mineralization is also widely used to examine the biomechanical properties of bone. Since Raman spectroscopy is a non-invasive technique, the spectra of bone tissue can be observed without sample degradation and is therefore becoming increasingly popular for use in Tissue engineering (50).

3.1 Bone composition

Bone has a complex hierarchical structure, and consists of a varied organization of material structures which work together to perform diverse mechanical, biological, and chemical functions at many length scales (51). The hierarchical structure is an irregular

arrangement; hence the material of bone is both heterogeneous and anisotropic. Bone has many functions; it acts as a protection for cells and organs, performs mineral ion homeostasis, and provides structural support (52).

It is important to understand the various levels of hierarchical structure when discussing bone quality. Firstly, the macrostructure (which can be measured by conventional mechanical testing), consists of trabecular and cortical bone (51). All bone is structurally organised into trabecular or cortical bone depending on its function. Trabecular bone is typically spongy and cancellous, and has a much greater metabolic turnover than cortical bone due to its high surface area for cellular activity. Cortical bone is dense and compact, and has a much greater mass than trabecular bone (53).

The most common type of cortical bone is haversian, which can be studied by imaging a sample at the microstructural level. It is composed of a complex arrangement of haversian systems, osteons, and single trabeculae. Vascular channels are surrounded by lamellar bone, and the complex arrangement of lamellae around the vascular channel is called an osteon (54). Single lamellae can be observed by imaging at the sub-microstructural level.

Structural information at the nano and sub-nanostructural levels is obtained via Raman spectroscopy. Bone nanostructures consist of mineral, collagen, and non-collagenous organic proteins (51). The mineral component of bone is observed in the form of small crystals in the shape of needles, plates and rods. These crystals are located inside and between a network of polymeric proteins (primarily type I collagen fibres), and consist of largely impure Hydroxyapatite ($CA_{10}(PO)_4OH_2$). The impure Hydroxyapatite contains constituents such as citrate, magnesium, carbonate, fluoride and strontium. The crystals are hard and stiff and therefore act as structural reinforcement to the collagen (55). Thus knowing the amount of mineral present in the bone is important in order to determine its mechanical stiffness and strength.

3.2 Bone quality

Bone quality (often referred to as intrinsic bone material properties) is determined by assessing the amount, and quality, of bone mineral (56). The crystal properties of the material can alter the bone strength and mechanical stiffness. An example of this is Osteoporosis imperfecta where the matrix is defective, the crystals are abnormally small and deformed and are sometimes found outside of the collagen matrix (56). Raman spectroscopy can be used to provide information representative of the mineral amount, composition, and crystallinity non-destructively and with a high spatial resolution. Most importantly, information from the mineral and organic components of bone can be obtained simultaneously, creating a complete picture of the composition of the bone sample (6).

The degree of mineralization of a bone sample is most commonly used to determine its quality. Raman spectra obtained from a sample provide information which can determine the degree of mineralization of the collagen matrix (the mineral/matrix ratio). Specific bands used to determine the degree of mineralization are; the phosphate ν_1 band at approximately 960cm^{-1} , and all of the bands associated with collagen (Amide III $\sim 1250\text{cm}^{-1}$, $\text{CH}_2 \sim 1450\text{cm}^{-1}$, C-H stretch $\sim 2800\text{cm}^{-1}$ and Amide I at approximately 1665cm^{-1}) (34). The Amide bands are particularly good indicators of protein conformation due to their sub-structural role in cross-linking and bonding (57).

The relative amounts of organic matrix and mineral crystals provide valuable bone quality information. The mineral to matrix ratio is obtained by calculating the ratio of peak heights of the integrated areas, for any of the aforementioned phosphate or amide peaks. There is disagreement amongst the literature as to which bands should be used to determine the mineral-to-matrix ratio (6, 34, 58, 59). This is because some amide and phosphate bands are more sensitive to the orientation and polarization of the incident light than others.

3.2 Orientation effects and the assessment of bone quality

Distinguishing between orientation and compositional contribution to the Raman spectrum is essential as mineral collagen fibres have different orientation within successive lamellae (58). Therefore the Raman bands least affected by orientation and the polarization of the incident light should be used to determine the mineral/matrix ratio.

Laser excitation induces a polarization in the sample which is parallel to the incident electric field. If a vibration is totally symmetric, the scattered photons will have the same polarization as the excitation source. Hence the intensity of observed photons is heavily dependent on the observation direction (18). This indicates that Raman bands are sensitive to polarization angle. The Raman sensitivity as a function of polarization angle must be determined in order to obtain structural and chemical information. Several authors have also reported a stronger polarization dependence according to the age of the bone sample (18, 58).

The effect of orientation on Raman bands which are most commonly used to obtain a mineral to matrix ratio may lead to erroneous conclusions (namely phosphate ν_1 , amide I and amide III bands). The phosphate ν_1 band represents the amount of bone mineral present, and the amide I/ III collagen bands are representative of the sample's organic component. The amide III band is mainly associated with the C-N vibration, and the amide I mode originates from the C=O stretching vibration. Amide I (C=O stretching) bands are parallel to the collagen backbone and are reliant on the orientation of the collagen. The two bands display two entirely different polarization behaviours and therefore cannot be expected to give the same result.

In a study by Gamsjaeger *et al* (58), the intensity of the Amide I band is shown to increase in the vertical section when the angle between the samples longitudinal axis and the polarization direction of the laser is changed. This confirms the dependency of the amide I band on the polarization orientation of the incident light. Gamsjaeger *et al* also report a strong variation of the PO_4 /amide I peak ratio when the angle of the laser beam polarization

is altered. When the laser excitation was depolarized, the variation vanished. This confirms that the variation is due to c-axis collagen orientation and the polarization orientation of the incident light, and that the exclusive use of a $\nu_1 PO_4$ /amide I peak ratio can lead to erroneous conclusions.

Since the $\nu_1 PO_4$ /amide I peak ratio is dependent on tissue orientation, other peaks must be considered. The amide III band is mainly influenced by the C-N stretching vibrational mode. It has two components; one parallel to the C=O axis and the other parallel to the mineral c-axis. Therefore, unlike the $\nu_1 PO_4$ or the amide I peak, it has two vibrational modes and is not dependant on the orientation of the sample. The $\nu_2 PO_4$ and $\nu_3 PO_4$ bands also have two vibrational modes and the same argument applies. This is conclusive evidence that a mineral to matrix ratio based on the $\nu_2 PO_4$ /amide III or $\nu_3 PO_4$ /amide III peaks is less likely to be affected by orientation. The assessment of the degree of mineralization obtained using these peaks will therefore contribute to extremely accurate conclusions.

The substitution of carbonate ions into locations of phosphate ions or hydroxyl positions of the mineral crystals is the second contributing factor to bone quality. Small impurities in the mineral crystal are caused by carbonate substitution (53). Carbonate presence can alter the physical properties of the crystal, such as solubility, and the amount of substitution depends on the chemical and environmental history of the bone sample (34). The change in physical properties can cause critical biological effects and may influence the mechanical strength and structure of the bone (53).

Raman spectroscopy also enables the analysis of carbonate substitution. The ratio of intensities of the carbonate and phosphate symmetric stretch bands is used to calculate type B carbonate substitution (59). Type-B is the substitution of carbonate ions into the location of phosphate ions (60, 61) and has a relatively high Raman intensity. Type-A is the substitution of carbonate ions into hydroxyl positions. Its Raman intensity is extremely weak and is therefore often disregarded.

Mineral crystallinity is the third and final application of Raman spectroscopy used to assess bone quality. Mineral crystallinity is the shape and stoichiometry of the mineral crystals, and is affected by the thermodynamic and kinetic equilibrium of its surrounding environment (52, 62). Small changes in the structure of crystals can affect the mechanical properties of bone (63). Mineral crystallinity can be determined using the ν_1 phosphate band alone. The band width at half peak intensity is used such that $1/\text{band width} = \text{crystallinity}$. A greater crystallinity (a well-ordered crystal lattice) is indicated by a decreasing band width (34).

Currently, a patient's bone mineral density (BMD) is used to determine skeletal fragility due to ageing or bone disease. However there is controversy as to whether BMD can be relied upon to assess fracture risk, or whether the quality of bone should also be considered. The assumption that fragility depends only on the mass of the bone may be over-simplistic and outdated.

Although there is a strong correlation between decreased bone mass and osteoporotic fractures, BMD cannot be used to determine if an individual will sustain fracture without supplementary information (64). As previously discussed there are a number of factors which influence the strength of bone, its quality, and its fracture susceptibility. There is therefore substantial evidence to suggest that bone quality should also be considered.

The use of BMD alone has a fracture detection rate of 35-50%, and a false positive rate of 15% (65). The opportunity to improve the accuracy of the prediction of fracture risk and the diagnosis of degenerative bone diseases is therefore immediately apparent. Raman spectroscopy provides excellent bone quality information and could be used to determine the quality of a small bone biopsy and improve fracture detection rate in the future.

4 Equipment selection

There are extensive variations in the choice of Raman spectroscopy equipment. In the study of bone composition, the impact of several equipment choices is often discussed, however to date there is no “golden standard” equipment setup.

As an example, Raman micro-spectrometers are often employed for the study of bone composition by biologists and in medical research (66-69). Micro spectrometers can have a microscope easily coupled to, or inherently part of dispersive instrumentation (12). Scattered radiation is focused by the microscope onto the detector. The purpose of a microscope is to enable the user to analyse microscopic samples or a microscopic areas of a larger sample.

However, obtaining a spectrum which may be inhomogeneous at the microscopic level is difficult. Bone is heterogeneous and therefore single point Raman microscopy cannot adequately describe its chemical microstructure (5) and spatial information is needed. This results in the spectrum obtained from one area of the bone being considerably different to that of another area. This is just one example of how poor equipment selection can affect the reliability of results and presents an opportunity for further research into the optimum equipment combination for the Raman imaging of bone.

4.1 Laser selection

Laser excitation sources are the most widely disputed choice of equipment, and there is currently no agreement as to the optimum wavelength for bone imaging. The intensity of Raman scattering is proportional to the frequency of the incident laser light (11) which suggests that in order to improve Raman sensitivity, a high frequency laser should be used. Laser excitation sources with wavelengths in the visible and near-Infrared (hereafter referred to as NIR) ranges are most commonly used, and NIR is extensively used for modern studies of biological samples. Using deep red excitation eliminates most fluorescence and allows weak organic matrix bonds to be seen clearly (34, 41, 42). NIR diffuse reflectance can be used to measure the Raman spectra of powdered samples with minimum sample preparation. It is also

extremely useful for quantitative analysis since smaller absorptivity's and lower scattering coefficients (at shorter wavelengths) result in a larger ratio of scattering to absorption (70).

Despite this, extensive research into the literature surrounding the Raman spectra of phosphate vibrational and OH stretch modes of Hydroxyapatite [(2, 35, 61, 71-76), Table 1] reveals that the spectra is largely unaffected by the wavelength or power of the laser excitation source. This is an interesting result as there are a number of factors detailed in previous literature (11-14, 19-23) that suggest the accuracy of a spectrum is affected by the choice of excitation source.

As with any experimental data there is slight variance in the spectra observed by different authors; however there is no trend relating laser power or wavelength to the difference in wavenumbers of shift. The $\nu_1 PO_4^{3-}$ vibrational and the OH stretch modes remain the most consistent, being reported at approximately 962 cm^{-1} and 3573 cm^{-1} respectively with no real anomalies. This is likely due to the fact that the $\nu_1 PO_4^{3-}$ band is the most intense on the spectrum, and is therefore often used for calibration of equipment and normalization (77).

As can be observed in table 1, from 1971 to present, excitation sources of increasing wavelengths have been employed. Recently published research rarely reports a laser source with a wavelength less than 785nm (78-82). This is undoubtedly due to technological advances in developing high power lasers; however in using a longer wavelength Raman sensitivity is reduced. Therefore high power lasers should be considered carefully before their integration into a Raman spectrometer.

	λ = unknown	λ = 488 or 515 nm	λ =514.5nm	λ =515nm	λ =515 and 632 nm	λ = 632nm	λ = 515 nm	λ = 785nm	λ =1064nm
Mode	Blakeslee 1971 [b]	Oshna 1974 [a]	walters 1990 [c]	Tsuda 1994 [d]	Penel 1996 [e]	Penel 1998 [f]	Saeii 2003 [g]	Dudek 2009 [h]	Konoyannis 2012 [i]
v2 PO4	431	436	451	432	433	432	470	432	430
	447			449	448	452		443	
				454					
v4 PO4	581	585		581	580	584	565	577	590
	592	597		593	591	590	571	590	
	608	613		609	607	611		604	
		621		617	614				
v1 PO4	962	968	961	962	963	961	962	959	961
	1031	1033		1028	1029	1032	1040	1028	
v3 PO4	1048	1052		1034	1034	1044	1070	1042	
	1078	1081		1043	1041	1071			
				1048	1048				
				1055	1057				
				1077	1064				
					1077				
OH stretch	3573	3573	Not observed	3572	3573	Not observed	3570	Not observed	Not observed

Table 1. Phosphate vibrational and OH stretch modes of hydroxyapatite as reported by multiple authors. The excitation wavelengths and year of publication are shown.

- [a] Argon ion laser with unspecified wavelength.
[b] Argon ion laser. Wavelength 488 or 515nm. Power output 200 to 500 mW.
[c] Argon ion laser. Wavelength 515nm. Power output 10 to 150mW.
[d] Argon ion laser. Wavelength 515nm. Power output unknown.
[e] OMARS89 micro spectrometer with helium neon laser excitation. Wavelengths 515 and 632nm. Power output 3mW.
[f] OMARS89 micro spectrometer with helium neon laser excitation. Wavelength 632nm. Power output 3mW.
[g] Argon ion laser. Wavelength 515nm. Power output 20mW.
[h] Wavelength 785nm. Power output 50mW.
[i] ND:YAG laser. Wavelength 1064nm. Power output 300mW.
[j] ND:YAG laser. Wavelength 1064nm. Power output 300mW.

Blakeslee, O'Shea, Walters, Tsuda, and Saeri *et al* (2, 35, 73, 75, 76), use Argon – ion lasers. This is a gas laser based on atomic transitions, and has a well-defined and narrow laser wavelength. The operating wavelength of Argon-ion lasers is not affected by environmental factors or optical alignment (83) which ensures it is simple to set up and operate.

Konstantinos *et al* (72) on the other hand employ a Nd:YAG laser excitation source which, like diode lasers, does not have a well-defined and narrow wavelength. Diode lasers often have the laser frequency locked by external cavity stabilization to a fixed value (84-86). Nd:YAG lasers are not frequency stabilized despite their lasing frequency being temperature dependent. A Nd:YAG laser has a $0.09 \text{ cm}^{-1} \text{ }^{\circ}\text{C}^{-1}$ shift with temperature (87) which can cause substantial errors resulting from large room temperature changes or inadequate warm up time. However, the Nd:YAG is a solid state laser and is therefore more electrically efficient than the Argon-Ion lasers which generate large heat dissipation and place huge demand on air cooling systems. It also emits light in the near infrared region, therefore the probability of exciting fluorescence in bone approaches zero (38).

Penel *et al* (61, 74) employ a Helium-Neon laser with wavelengths of 515 and 632 nm. This type of laser is popular for its high continuous use lifetime and low cost (14). The spectral region resulting from the 632nm excitation is near perfect for CCD detectors. However, the wavelengths 515 and 632nm are not long enough to completely avoid fluorescence background problems when illuminating Hydroxyapatite. A wavelength of 515nm improves Raman sensitivity but further increases fluorescence background.

The spectra reported by Saeri *et al* in 2003 stand out the most in comparison to the literature detailed in table 1. A $\nu_2 \text{ PO}_4^{3-}$ band was observed at 470 cm^{-1} , 16 cm^{-1} away from bands reported in other literature. Saeri *et al* also present $\nu_4 \text{ PO}_4^{3-}$ bands at 565 and 571 cm^{-1} , which are not within error of other accepted bands. The group employ an Argon-Ion laser for the study which is easily operated, however the laser operates at a wavelength of 514nm and could present fluorescence problems. Fluorescence is unlikely to account for an

error this large and it is likely to be experimental due to either equipment or to incorrect band assignments.

In conclusion, an exhaustive literature review reveals that the effects of laser selection are largely insignificant in relation to Hydroxyapatite, providing the light is not absorbed by either the sample or by impurities in the sample. The Raman spectrum of Hydroxyapatite remains unchanged in studies by several authors [as shown in table 1] who employ lasers with various wavelengths in the visible, ultraviolet and near infrared ranges. The slight differences in specific band positions do not show any trend with regards to laser gas, power, or wavelength and are likely to be due to real differences in the samples used. It can hereby be deduced that for modern studies, although NIR lasers are most commonly used, a laser in the visible or UV ranges will not dramatically affect the results. There is however an opportunity for further research into how laser selection affects the spectra of other materials.

5 Band assignments of Hydroxyapatite Raman spectra

As previously discussed, bone is composed of a mineral part, an organic matrix, and water (15). Hydroxyapatite is the mineral component of bone and is composed of Phosphate and Calcium. It forms approximately 65% of adult bone (16) and is a major component of human tooth enamel. Hydroxyapatite is bioactive and can be used to integrate into bone structures within the human body. It is therefore of great interest to the fields of tissue engineering and medicine.

Many recent tissue engineering studies which rely on Raman spectroscopy refer to major band assignments of Hydroxyapatite having been previously reported (8, 75, 88, 89). This introduces several questions such as; when and by whom the original band assignments were made, why are they so widely accepted to be true, and what is the threat to the field of tissue engineering if the original band assignments are shown to be incorrect?

As an example, McCredie *et al* (88) use Raman spectroscopy to examine the compositional differences in the bone tissue of women with and without osteoporotic fracture.

The authors conclude that there is a difference in the composition of iliac crest cortical bone between the two sample groups. The study relies on previously determined band assignments and uses the band intensities as an empirical measure of ratio. The band assignments referred to are reported by Carden and a Morris (34) who present a table of band assignments observed using both infrared and Raman, and give range of “accepted values”. However, the range provided is large and there is no reference detailing where these assignments were made, therefore their authenticity must be questioned. This is a possible threat to the work of McCredie *et al* as the band assignments have been accepted to be true without further questioning their origin.

5.1 Tracing original band assignments

A large selection of modern publications refer to Penel *et al* (1998 (61)) when discussing their Raman spectra and corresponding band assignments (43, 67, 90-94). This study reports the use of Raman spectroscopy to study the carbonate and phosphate vibrational modes of several synthetic and biological carbonated apatites. Their spectrum is then compared with that of hydroxyapatite, with the aim of specifying band assignments and spectral alterations due to carbonate incorporation and crystallinity. The paper includes a comprehensive table detailing band assignments for a number of biological and synthetic apatites. However there is little explanation as to how the band assignments were made, and the authors refer to a previous paper published in 1996 (74) and to Nishino *et al* (95).

In the aforementioned study by Penel *et al* (1996 (74)), Infrared and Raman micro spectroscopy have been used to investigate fluor-fluor-hydroxy and hydroxyapatite powders. An interesting conclusion presented by this paper is that the number of Raman or Infrared bands observed is always less than the number calculated or expected. In fact, this result can be seen in table 1 where the number of Raman active bands observed by several authors are inconsistent. With regards to the band assignments, the authors compare their own spectra with that of Klee (96) and Kravitz *et al* (1), with reference to O’Shea *et al* (73).

Furthermore, Nishino *et al* (95) use Raman spectroscopy to study Human tooth enamel. Raman was used alongside X-ray diffraction and Infrared spectroscopy to provide complementary information about the substitution of CO_3^{2-} in the enamel apatite. Nishino lists the frequencies of the observed spectrum in a table “where assignments of all the frequencies were made by comparison with previous Infrared and Raman data” (95). It is here that Nishino has also referred to O’Shea *et al* (73).

Thus far, references in modern tissue engineering papers with regards to Hydroxyapatite band assignments have led to Penel *et al* (1998, (61)). Penel refers to a previous paper published by the same authors in 1996 (74) and to Nishino *et al* (95), both of whom refer to O’Shea *et al* (73) as justification of their band assignments.

O’Shea *et al* (73) use spectroscopy to study the composition of several apatites. Although laser Raman studies of chlorapatite (CLAp), fluorapatite (FAP), and hydroxyapatite (OHAp) have been previously reported, O’Shea *et al* focus mainly on the spectral features which may serve as analytical tools for cross-section assays. This is also the first successful observation of the Raman spectra of (FOH)Ap and (ClOH)Ap mixed crystals and is therefore a significant contributor to the understanding of modern Raman spectroscopy. The spectral lines are detailed in a table with band assignments “known or herein deduced” (73). The spectra of fluorapatite is compared with that previously reported by Kravitz *et al* (1) and Levitt *et al* (3). Hydroxyapatite spectra is compared with that of Blakeslee *et al* (2), and chloroapatite with Kravitz *et al* (1).

It is unclear exactly which band assignments are known and which are deduced by O’Shea. There are however several interesting differences in the spectra of the present study against its comparisons [Table 2]. Firstly, for fluorapatite, Kravitz and Levitt report their first PO_3^2 bands at 427 and 431cm^{-1} respectively whereas these bands were not observed by O’Shea. The spectra for fluoroapatite observed by O’Shea almost all have a higher wavenumber than those previously reported and there are a few gaps where bands were not observed. For

hydroxyapatite and chloroapatite the results are similar and the majority of band positions have a slightly larger wavenumber than those previously reported.

	Fluorapatite			Hydroxyapatite		Chlorapatite	
	KKM	LBC	OS	BC	OS	KKM	OS
v2 PO4	427	431	436	431	436	425	429
	440	445	450	447	451	441	445
	446	447	450	581	585	447	
v4 PO4	582	580	587	592	597	577	576
	590	590		608	613	586	586
	592		597		621	593	593
	605	605	612	655	655	613	616
	617	615	621		621	623	620
v1 PO4	966	965	967	962	968	959	964
	1034	1032	1036	1031	1033	1012	1018
v3 PO4	1041	1040	1044			1032	1034
	1054	1051	1055		1046	1038	1037
	1060	1061	1061	1048	1052		1044
	1082	1080	1083	1078	1081	1055	1061
OH stretch				3573	3573	1075	1080

Table 2: Raman spectra of phosphate vibrational and OH stretch modes of fluorapatite, hydroxyapatite, and chlorapatite as reported by O'Shea and compared with several other authors detailed below.

KKM = Kravitz, Kingsley and Mahan (1)

BC = Blakeslee and Condrate (2)

LBC = Levitt, Blakeslee and Condrate (3)

Table 2 shows the Raman spectrum and its corresponding band assignments which are reported by O'Shea *et al* (73) for several apatites. There is a detailed description as to how the band assignments deduced by O'Shea *et al* were made and this is therefore the earliest paper which does not blindly reference previous band assignments. However, the band assignments deduced by O'Shea *et al* were for Fluorapatite and Chlorapatite. Since the primary concern of this chapter is Hydroxyapatite spectra, all other apatites are ignored from this point.

Blakeslee and Condrante (2) study the Raman spectra of hydrothermally prepared Hydroxyapatite. The previous band assignments for several mineralogical halogen-substituted apatites, determined using infrared spectroscopy, were found to be incorrect by Levitt and Condrante (97) and so the assignments for Hydroxyapatite were assumed to be incorrect by analogy. The band assignments for strontium Hydroxyapatite are similarly speculative and have been assigned using Infrared with no complementary Raman spectra. Blakeslee and Condrante (2) are the first to observe the Raman spectra of Barium and Lead hydroxyapatites. Since Calcium Hydroxyapatite best describes the mineral phase in bone and teeth, it is most relevant to this project. Therefore the band assignments of strontium, barium and lead hydroxyapatites are not currently of interest.

A previous attempt to observe the Raman spectra of calcium hydroxyapatite was made by Levitt *et al* (3), however the presence of impurities created fluorescence problems that made it impossible to observe any spectra besides the strongest fundamental mode. Therefore the band assignments made by Levitt *et al* are speculative without the observation of the full Raman spectra. Blakeslee *et al* (2) are the first to successfully observe the Raman spectrum of hydroxyapatite, and this paper is therefore the origin of band assignments.

5.2 The reliability of original band assignments

Blakeslee *et al* (2) are the first to successfully observe the laser-Raman spectra of calcium hydroxyapatite without fluorescence problems. Although its Infrared spectra had been previously reported by several authors (3, 33, 98, 99), these band assignments are likely to be

incorrect without complementary Raman spectra (100). The spectrum reported by Blakeslee *et al* is shown in the paper and displays well defined peaks at all of the phosphate vibrational and OH stretch modes. Band assignments were made according to these spectra when complimented by that of the middle-infrared region. The most intense observable band at 962 cm^{-1} which represents the total symmetrical stretching frequency is assigned to $PO_4^{3-} \nu_1$ in agreement with other authors in both infrared and Raman. The assignments of the 447 and 431 cm^{-1} bands to the $PO_4^{3-} \nu_2$ mode are consistent with the previously referred to study by Levitt and Condrante (97) which predicts that the $PO_4^{3-} \nu_2$ mode must occur above 400 cm^{-1} . The 581, 592 and 608 cm^{-1} components are assigned to the $PO_4^{3-} \nu_4$ mode.

The Raman band assignments have been made by simply comparing the positions of the bands to those observed by other authors in the Infrared range. As Blakeslee *et al* are the first to view a complete Raman spectrum of hydroxyapatite, there is no Raman data to compare with and so the band assignments are tentatively made.

There are a number of discrepancies in the presented infrared data used for comparison. Firstly for the $PO_4^{3-} \nu_3$ mode, Elliot *et al* (98) and Stutman *et al* (99) failed to observe a band, whereas others observed bands at 350, 350, 473, and 470 cm^{-1} (2, 3, 33, 101). The range in observed values is significant (120 cm^{-1}) and suggests that one or more of the peaks has been incorrectly assigned to the $PO_4^{3-} \nu_3$ mode. Another example is the $PO_4^{3-} \nu_3$ mode where one particular peak was observed at various points between 1048 and 1074 cm^{-1} which gives a range of 26 cm^{-1} and cannot be accurately relied upon.

Many of the sources of infrared band assignments which have been used as a tool for comparison also have an extremely tentative approach to band assignments. Fowler (33) was among the first to observe the infrared spectra of Hydroxyapatite and concludes that “probable band assignments are given” (33). The lack of confidence in their band assignments demonstrated by the authors is extremely worrying if the amount of modern research which rely on them is considered.

The band assignments made by Blakeslee are the first for Hydroxyapatite in the Raman spectral range, and have been made by comparison to inconsistent infrared peaks which have been previously reported. It is these band assignments upon which many modern tissue engineering, biology, and medicine papers are based. The band assignments have been widely referred to and used without question, and the threat to the entire field of tissue engineering is huge if the band assignments are found to be inaccurate. There is therefore an urgent need for the original band assignments to be reviewed.

Discussion

Although the Raman spectrum of bone is frequently studied, no research into its reliability exists. The aim of this literature review was to assess the reliability of Raman spectroscopy and its equipment when applied to the study of bone composition.

There is currently an opportunity to improve fracture detection rate and the diagnosis of degenerative bone diseases. The assessment of bone quality as well as BMD may prove to be extremely useful to assess the mechanical strength and hardness of bone samples. However, the $\nu_1 PO_4$ /amide I peak ratio which is commonly used to determine mineral crystallinity, is dependent on tissue orientation which may lead to erroneous conclusions. The $\nu_2 PO_4$ /amide III or $\nu_3 PO_4$ /amide III encompass two vibrational modes and are therefore less likely to be affected by tissue orientation. These bands are not currently used to calculate the mineral to matrix ratio in bone, despite providing increased accuracy.

Surprisingly and in contrast to other literature, the Raman spectra of Hydroxyapatite is shown to be unaffected by the wavelength, frequency, or power of the laser excitation source. However, there is an opportunity for further research into whether the spectrum of whole bone is affected by laser selection or even deproteinization.

The advantages of FT-Raman spectrometers outweigh its disadvantages, and the technique is shown to be superior to dispersive instrumentation in the study of bone. The organic matrix of bone has previously resulted in its Raman spectrum being masked by

fluorescence. FT-Raman has the ability to almost entirely eliminate fluorescence and is therefore a hugely beneficial technique and reduces the need for sample preparation.

Finally, the original band assignments for the Raman spectra of Hydroxyapatite were made with reservations in 1971 by Blakeslee *et al* (2). The band assignments were made by comparison with tentatively assigned infrared bands, and therefore cannot be relied upon for modern studies. Despite this, references provided by modern papers can be traced to the original assignments and no attempt has been made to review them. Since Hydroxyapatite is bioactive, it is currently of great interest to the fields of tissue engineering and medicine. The band assignments are blindly referenced in many studies, when in fact they are extremely unreliable. There is therefore an urgent need for the band assignments to be reviewed.

Several opportunities for future research can be identified. Firstly, an investigation into whether laser selection affects the spectra of organic components present in bone would be beneficial to future tissue engineering studies. The identification of a single laser which provides the most accurate spectrum would be extremely useful. Original band assignments of Hydroxyapatite spectra must be reviewed, and the reliability of the band assignments for other substances could be investigated.

References

1. KRAVITZ, L.C., J.D. KINGSLEY and E.L. ELKIN. RAMAN AND INFRARED STUDIES OF COUPLED PO₄-3 VIBRATIONS. *Journal of Chemical Physics*, 1968, **49**(10), pp.4600-&.
2. BLAKESLEE, K.C. and R.A. CONDRATE. Vibrational Spectra of Hydrothermally Prepared Hydroxyapatites. *Journal of the American Ceramic Society*, 1971, **54**(11), pp.559-563.
3. LEVITT S R, B.K.C., CONDRATE R A Infrared spectra and Laser-Raman spectra of several apatites *Mem. soc. r. sci. Liege*, 1971, pp.121-141.
4. YAMAMOTO, T., K. UCHIDA, K. NARUSE, M. SUTO, K. URABE, K. UCHIYAMA, K. SUTO, M. MORIYA, M. ITOMAN and M. TAKASO. Quality assessment for processed and sterilized bone using Raman spectroscopy. *Cell and Tissue Banking*, 2012, **13**(3), pp.409-414.
5. KAZANCI, M., P. ROSCHGER, E.P. PASCHALIS, K. KLAUSHOFER and P. FRATZL. Bone osteonal tissues by Raman spectral mapping: Orientation-composition. *Journal of Structural Biology*, 2006, **156**(3), pp.489-496.

6. CARDEN, A., R.M. RAJACHAR, M.D. MORRIS and D.H. KOHN. Ultrastructural changes accompanying the mechanical deformation of bone tissue: A Raman imaging study. *Calcified Tissue International*, 2003, **72**(2), pp.166-175.
7. CALLENDER, A.F., W.F. FINNEY, M.D. MORRIS, N.D. SAHAR, D.H. KOHN, K.M. KOZLOFF and S.A. GOLDSTEIN. Dynamic mechanical testing system for Raman microscopy of bone tissue specimens. *Vibrational Spectroscopy*, 2005, **38**(1-2), pp.101-105.
8. DOPNER, S., F. MULLER, P. HILDEBRANDT and R.T. MULLER. Integration of metallic endoprotheses in dog femur studied by near-infrared Fourier-transform Raman microscopy. *Biomaterials*, 2002, **23**(5), pp.1337-1345.
9. LOPES, C.B., A.L.B. PINHEIRO, S. SATHAIAH, N.S. DA SILVA and M.A.C. SALGADO. Infrared laser photobiomodulation (λ 830 nm) on bone tissue around dental implants: A Raman spectroscopy and scanning electronic microscopy study in rabbits. *Photomedicine and Laser Surgery*, 2007, **25**(2), pp.96-101.
10. VAN APELDOORN, A.A., Y. AKSENOV, I. HOFLAND, J.D. DE BRUIJN, C. OTTO, J. GREVE and C.A. VAN BLITERSWIJK. Combined confocal Raman spectroscopy and scanning electron microscopy reveal early in vitro bone formation is comparable to organized mature bone. *Tissue Engineering*, 2003, **9**(4), pp.844-844.
11. ANDERSON, A. *The Raman Effect*. Waterloo Canada Marcel Dekker INC, 1971.
12. EWEN SMITH, G.D. *Modern Raman Spectroscopy, a practical approach* West Sussex John Wiley & Sons 2005.
13. FREEMAN, S. *Applications of laser Raman spectroscopy*. Canada Wiley & sons inc, 1974.
14. SZYMANSKI, H. *Raman spectroscopy: theory and practice* New York Plenum Press, 1967.
15. ROACH, H.I. Why does bone matrix contain non-collagenous proteins? The possible roles of osteocalcin, osteonectin, osteopontin and bone sialoprotein in bone mineralisation and resorption. *Cell Biology International*, 1994, **18**(6), pp.617-628.
16. NSBRI. *Bone development and structure* [online]. 2005. [Accessed].
17. MORRIS, M.D. Raman assessment of bone quality. *clinical orthopaedics*, 2011, **469**(8), pp.2160-2169.
18. MCCREERY, R.L. Raman Spectroscopy for Chemical Analysis. *Measurement Science and Technology*, 2001, **12**(5), p.653.
19. LONG, D. *The Raman Effect* West Sussex Wiley & Sons Ltd, 2003.
20. J.R FERRARO, K.N. *Introductory Raman Spectroscopy* Academic Press. San Diego 2004.
21. PELLETIER, M. *Analytical Applications of Raman spectroscopy* Michigan USA Blackwell sciences ltd 1999.
22. TOBIN, M. *Laser Raman Spectroscopy* Connecticut Wiley & sons inc 1971.
23. LONG, D. *Raman spectroscopy* Great Britain McGrawn Inc 1977.
24. SHARMA, B., S.V. BYKOV and S.A. ASHER. UV resonance Raman investigation of electronic transitions in alpha-helical and polyproline II-like conformations. *Journal of Physical Chemistry B*, 2008, **112**(37), pp.11762-11769.
25. ESMONDE-WHITE, K. *Raman spectroscopy detection of molecular hanges associated with osteoarthritis* Doctor of philosophy thesis, University of Michigan 2009.
26. J FERRARO, K.N. *Introductory Raman spectroscopy* San Diego Academic press INC 1994.

27. HAMMOND, C. *The basics of crystallography and diffraction* Leeds: Oxford University press 2009.
28. TKACZYK, T.S. *A field guide to microscopy* Society of Photo-Optical Instrumentation Engineers, 2010.
29. SHAW, A.D., N. KADERBHAI, A. JONES, A.M. WOODWARD, R. GOODACRE, J.J. ROWLAND and D.B. KELL. Noninvasive, On-Line Monitoring of the Biotransformation by Yeast of Glucose to Ethanol Using Dispersive Raman Spectroscopy and Chemometrics. *Applied Spectroscopy*, 1999, **53**(11), pp.1419-1428.
30. CHANTRY, G.W., H.A. GEBBIE and C. HILSUM. INTERFEROMETRIC RAMAN SPECTROSCOPY USING INFRA-RED EXCITATION. *Nature*, 1964, **203**(494), pp.1052-&.
31. AGARWAL, U. FT-Raman spectroscopy: what is it and what can it do for reasearch on ligocellulosic materials *In: 8th international symposium on wood and pulping chemistry* Helsinki, Finland Proceedings, 1995, pp.67-72.
32. HIRSCHFELD, T. and B. CHASE. FT-Raman Spectroscopy: Development and Justification. *Appl. Spectrosc.*, 1986, **40**(2), pp.133-137.
33. FOWLER, B.O. Infra-red spectra of hydroxyapatite, octacalcium phosphate, and pyrolysed octacalcium phosphate *Archives of Oral Biology*, 1966, **11**(5), pp.447-492.
34. CARDEN, A. and M.D. MORRIS. Application of vibrational spectroscopy to the study of mineralized tissues (review). *Journal of Biomedical Optics*, 2000, **5**(3), pp.259-268.
35. WALTERS, M.A., Y.C. LEUNG, N.C. BLUMENTHAL, R.Z. LEGEROS and K.A. KONSKER. A RAMAN AND INFRARED SPECTROSCOPIC INVESTIGATION OF BIOLOGICAL HYDROXYAPATITE. *Journal of Inorganic Biochemistry*, 1990, **39**(3), pp.193-200.
36. B Z GEVORKYAN, N.Y.A., Y N FEDORA Study or the structure of bone tissue using the polarized spectra of combination scatter *Biofizica*, 1984, **29**, pp.1140-1148.
37. CARTER, D.H., A.J. SCULLY, D.A. HEATON, M.P.J. YOUNG and J.E. AARON. Effect of deproteination on bone mineral morphology: implications for biomaterials and aging. *Bone*, 2002, **31**(3), pp.389-395.
38. D CHASE, J.R. *Fourier transform Raman spectroscopy: from concept to experiment* London Acedemic press INC, 1994.
39. ANTOLASIC, F. *The advantages of FT-spectroscopy* [online]. 2009. [Accessed 05th December]. Available from: <http://minyos.its.rmit.edu.au/~rcmfa/FTIR/advant.htm>.
40. COMPSTON, J. *The structure of bone* medicine international. Oxford Medical education 1994.
41. SMITH, R. and I. REHMAN. FOURIER-TRANSFORM RAMAN-SPECTROSCOPIC STUDIES OF HUMAN BONE. *Journal of Materials Science-Materials in Medicine*, 1994, **5**(9-10), pp.775-778.
42. REHMAN, I., R. SMITH, L.L. HENCH and W. BONFIELD. STRUCTURAL EVALUATION OF HUMAN AND SHEEP BONE AND COMPARISON WITH SYNTHETIC HYDROXYAPATITE BY FT-RAMAN SPECTROSCOPY. *Journal of Biomedical Materials Research*, 1995, **29**(10), pp.1287-1294.
43. MORRIS, M.D. and G.S. MANDAIR. Raman Assessment of Bone Quality. *Clinical Orthopaedics and Related Research*, 2011, **469**(8), pp.2160-2169.
44. OKAGBARE, P.I., D. BEGUN, M. TECKLENBURG, A. AWONUSI, S.A. GOLDSTEIN and M.D. MORRIS. Noninvasive Raman spectroscopy of rat tibiae: approach to in vivo assessment of bone quality. *Journal of Biomedical Optics*, 2012, **17**(9).

45. BUCKLEY, K., P. MATOUSEK, A.W. PARKER and A.E. GOODSHIP. Raman spectroscopy reveals differences in collagen secondary structure which relate to the levels of mineralisation in bones that have evolved for different functions. *Journal of Raman Spectroscopy*, 2012, **43**(9), pp.1237-1243.
46. ESMONDE-WHITE, K.A., J. SOTTNIK, M. MORRIS and E. KELLER. Raman spectroscopy of bone metastasis. In: N. KOLLIAS, *et al.*, eds. *Photonic Therapeutics and Diagnostics Viii, Pts 1 and 2*. 2012.
47. PASCHALIS, E.P., A. VAN LIEROP, R. VAN BEZOOIJEN, S. GAMSJAEGER, B. HOFSTETTER, A. ROSCHGER, P. ROSCHGER, K. KLAUSHOFER and S.E. PAPAPOULOS. Sclerosteosis patients have altered intrinsic bone material properties as assessed by Raman spectroscopy. *Bone*, 2012, **51**(6), pp.S13-S14.
48. BUCHWALD, T., K. NICIEJEWSKI, M. KOZIELSKI, M. SZYBOWICZ, M. SIATKOWSKI and H. KRAUSS. Identifying compositional and structural changes in spongy and subchondral bone from the hip joints of patients with osteoarthritis using Raman spectroscopy. *Journal of Biomedical Optics*, 2012, **17**(1).
49. MEDICINE, U.N.L.O. *Bone Diseases* [online]. 2012. [Accessed 05/12/2012].
50. NOTINGHER, I., S. VERRIER, H. ROMANSKA, A.E. BISHOP, J.M. POLAK and L.L. HENCH. In situ characterisation of living cells by Raman spectroscopy. *Spectroscopy-an International Journal*, 2002, **16**(2), pp.43-51.
51. RHO, J.Y., L. KUHN-SPEARING and P. ZIOUPOS. Mechanical properties and the hierarchical structure of bone. *Medical Engineering & Physics*, 1998, **20**(2), pp.92-102.
52. BOSKEY, A.L. Variations in bone mineral properties with age and disease. *Journal of Musculoskeletal & Neuronal Interactions*, 2002, **2**(6), pp.532-534.
53. J BUCKWALTER, T.E., S SIMON *Orthopaedic basic science: Biology and Biomechanics of the musculoskeletal system USA* American academy of Orthopaedic surgeons 2000.
54. COWIN, S. *Bone Mechanics: Handbook* New York Informa healthcare USA 2009.
55. BARTH, H.D., E.A. ZIMMERMANN, E. SCHAIBLE, S.Y. TANG, T. ALLISTON and R.O. RITCHIE. Characterization of the effects of x-ray irradiation on the hierarchical structure and mechanical properties of human cortical bone. *Biomaterials*, 2011, **32**(34), pp.8892-8904.
56. CAMACHO, N.P., L. HOU, T.R. TOLEDANO, W.A. ILG, C.F. BRAYTON, C.L. RAGGIO, L. ROOT and A.L. BOSKEY. The material basis for reduced mechanical properties in oim mice bones. *Journal of Bone and Mineral Research*, 1999, **14**(2), pp.264-272.
57. BANDEKAR, J. AMIDE MODES AND PROTEIN CONFORMATION. *Biochimica Et Biophysica Acta*, 1992, **1120**(2), pp.123-143.
58. GAMSJAEGER, S., A. MASIC, P. ROSCHGER, M. KAZANCI, J.W.C. DUNLOP, K. KLAUSHOFER, E.P. PASCHALIS and P. FRATZL. Cortical bone composition and orientation as a function of animal and tissue age in mice by Raman spectroscopy. *Bone*, 2010, **47**(2), pp.392-399.
59. AKKUS, O., F. ADAR and M.B. SCHAFFLER. Age-related changes in physicochemical properties of mineral crystals are related to impaired mechanical function of cortical bone. *Bone*, 2004, **34**(3), pp.443-453.
60. FRUSHOUR, B.G. and J.L. KOENIG. RAMAN-SCATTERING OF COLLAGEN, GELATIN, AND ELASTIN. *Biopolymers*, 1975, **14**(2), pp.379-391.

61. PENEL, G., G. LEROY, C. REY and E. BRES. MicroRaman Spectral Study of the PO₄; and CO₄ ; Vibrational Modes in Synthetic and Biological Apatites. *Calcified Tissue International*, 1998, **63**(6), pp.475-481.
62. BOSKEY, A.L., M. MARESCA, W. ULLRICH, S.B. DOTY, W.T. BUTLER and C.W. PRINCE. OSTEOPOINTIN-HYDROXYAPATITE INTERACTIONS IN-VITRO - INHIBITION OF HYDROXYAPATITE FORMATION AND GROWTH IN A GELATIN-GEL. *Bone and Mineral*, 1993, **22**(2), pp.147-159.
63. YERRAMSHETTY, J.S. and O. AKKUS. The associations between mineral crystallinity and the mechanical properties of human cortical bone. *Bone*, 2008, **42**(3), pp.476-482.
64. BOYCE, T.M. and R.D. BLOEBAUM. CORTICAL AGING DIFFERENCES AND FRACTURE IMPLICATIONS FOR THE HUMAN FEMORAL-NECK. *Bone*, 1993, **14**(5), pp.769-778.
65. MARSHALL, D., O. JOHNELL and H. WEDEL. Meta-analysis of how well measures of bone mineral density predict occurrence of osteoporotic fractures. *British Medical Journal*, 1996, **312**(7041), pp.1254-1259.
66. DIPPEL, B., R.T. MUELLER, A. PINGSMANN and B. SCHRADER. Composition, constitution, and interaction of bone with hydroxyapatite coatings determined by FT Raman microscopy. *Biospectroscopy*, 1998, **4**(6), pp.403-412.
67. GOODYEAR, S.R. and R.M. ASPDEN. Raman Microscopy of Bone. In: M.H. HELFRICH and S.H. RALSTON, eds. *Bone Research Protocols, Second Edition*. 2012, pp.527-534.
68. MORRIS, M.D., A. CARDEN, R.M. RAJACHAR and D.H. KOHN. Bone microstructure deformation observed by Raman microscopy. In: T. VODINH, W.S. GRUNDFEST and D.A. BENARON, eds. *Biomedical Diagnostic, Guidance, and Surgical-Assist Systems Iii*. 2001, pp.81-89.
69. PENEL, G., C. DELFOSSE, M. DESCAMPS and G. LEROY. Composition of bone and apatitic biomaterials as revealed by intravital Raman microspectroscopy. *Bone*, 2005, **36**(5), pp.893-901.
70. BLUMICH, M. *IR spectroscopy* Germany Wiley-VCH, 2002.
71. DUDEK, A. Surface properties in titanium with hydroxyapatite coating. *Optica Applicata*, 2009, **39**(4), pp.825-831.
72. K. KONSTANTINOS, O.M., K.CHRISTOS Analysis of bone composition with Raman spectroscopy 2012.
73. O'SHEA, D.C., M.L. BARTLETT and R.A. YOUNG. Compositional analysis of apatites with Laser-Raman spectroscopy: (OH,F,Cl)apatites. *Archives of Oral Biology*, 1974, **19**(11), pp.995-1006.
74. PENEL, G., G. LEROY and C. REY. Raman study of synthetics and human enamel apatites. *Journal of Dental Research*, 1996, **75**(5), pp.1229-1229.
75. SAERI, M.R., A. AFSHAR, M. GHORBANI, N. EHSANI and C.C. SORRELL. The wet precipitation process of hydroxyapatite. *Materials Letters*, 2003, **57**(24-25), pp.4064-4069.
76. TSUDA, H. and J. ARENDS. ORIENTATIONAL MICRO-RAMAN SPECTROSCOPY ON HYDROXYAPATITE SINGLE-CRYSTALS AND HUMAN ENAMEL CRYSTALLITES. *Journal of Dental Research*, 1994, **73**(11), pp.1703-1710.
77. SERGO, V., O. SBAIZERO and D.R. CLARKE. Mechanical and chemical consequences of the residual stresses in plasma sprayed hydroxyapatite coatings. *Biomaterials*, 1997, **18**(6), pp.477-482.
78. WANG, Q., S.M. LONERGAN and C.X. YU. Rapid determination of pork sensory quality using Raman spectroscopy. *Meat Science*, 2012, **91**(3), pp.232-239.

79. LI, B., P.W. RYAN, B.H. RAY, K.J. LEISTER, N.M.S. SIRIMUTHU and A.G. RYDER. Rapid Characterization and Quality Control of Complex Cell Culture Media Solutions Using Raman Spectroscopy and Chemometrics. *Biotechnology and Bioengineering*, 2010, **107**(2), pp.290-301.
80. BOYD, A., G. BURKE and B. MEENAN. Monitoring cellular behaviour using Raman spectroscopy for tissue engineering and regenerative medicine applications. *Journal of Materials Science: Materials in Medicine*, 2010, **21**(8), pp.2317-2324.
81. BENNETT, M.D., C.J. WOLTERS, K.F. BRANDSTADT and M.M.J. TECKLENBURG. Raman spectroscopy and DFT calculations of intermediates in the hydrolysis of methylmethoxysilanes. *Journal of Molecular Structure*, 2012, **1023**, pp.204-211.
82. MAZUREK, S. and R. SZOSTAK. Quantitative analysis of thiamine hydrochloride in tablets—Comparison of infrared attenuated total reflection, diffuse reflectance infrared and Raman spectroscopy. *Vibrational Spectroscopy*, 2012, **62**(0), pp.10-16.
83. KARGER, A.M., R.P. ENGLISH and R.J.D. SMITH. Laser Raman Spectrometer for Process Control. *Appl. Opt.*, 1973, **12**(9), pp.2083-2087.
84. RICCI, L., M. WEIDEMULLER, T. ESSLINGER, A. HEMMERICH, C. ZIMMERMANN, V. VULETIC, W. KONIG and T.W. HANSCH. A COMPACT GRATING-STABILIZED DIODE-LASER SYSTEM FOR ATOMIC PHYSICS. *Optics Communications*, 1995, **117**(5-6), pp.541-549.
85. ANGEL, S.M., M. CARRABBA and T.F. COONEY. The utilization of diode lasers for Raman spectroscopy. *Spectrochimica Acta Part a-Molecular and Biomolecular Spectroscopy*, 1995, **51**(11), pp.1779-1799.
86. LANG, M. External-cavity designs satisfy stringent demands. *Laser Focus World*, 1996, **32**(6), pp.187-+.
87. KOECHNER, W. *Solid-state laser engineering* Berlin: Springer-Verlag, 1996.
88. MCCREADIE, B.R., M.D. MORRIS, T.-C. CHEN, D.S. RAO, W.F. FINNEY, E. WIDJAJA and S.A. GOLDSTEIN. Bone tissue compositional differences in women with and without osteoporotic fracture. *Bone*, 2006, **39**(6), pp.1190-1195.
89. NOTINGHER, I., J.R. JONES, S. VERRIER, I. BISSON, P. EMBANGA, P. EDWARDS, J.M. POLAK and L.L. HENCH. Application of FTIR and Raman spectroscopy to characterisation of bioactive materials and living cells. *Spectroscopy-an International Journal*, 2003, **17**(2-3), pp.275-288.
90. BELLUCCI, D., G. BOLELLI, V. CANNILLO, A. CATTINI and A. SOLA. In situ Raman spectroscopy investigation of bioactive glass reactivity: Simulated body fluid solution vs TRIS-buffered solution. *Materials Characterization*, 2011, **62**(10), pp.1021-1028.
91. MARKOVIC, S., L. VESELINOVIC, M.J. LUKIC, L. KARANOVIC, I. BRACKO, N. IGNJATOVIC and D. USKOKOVIC. Synthetical bone-like and biological hydroxyapatites: a comparative study of crystal structure and morphology. *Biomedical Materials*, 2011, **6**(4).
92. CAMPILLO, M., P.D. LACHARMOISE, J.S. REPARAZ, A.R. GONI and M. VALIENTE. On the assessment of hydroxyapatite fluoridation by means of Raman scattering. *Journal of Chemical Physics*, 2010, **132**(24).
93. MORRIS, M.D. Raman Spectroscopy of Bone and Cartilage. In: P. MATOUSEK and M.D. MORRIS, eds. *Emerging Raman Applications and Techniques in Biomedical and Pharmaceutical Fields*. 2010, pp.347-364.
94. BI, X., C. PATIL, C. MORRISSEY, M.P. ROUDIER, A. MAHADEVAN-JANSEN and J. NYMAN. Characterization of Bone Quality in Prostate Cancer Bone Metastases

- Using Raman Spectroscopy. In: N. KOLLIAS, *et al.*, eds. *Photonic Therapeutics and Diagnostics VI*. 2010.
95. NISHINO, M., S. YAMASHITA, T. AOBA, M. OKAZAKI and Y. MORIWAKI. THE LASER-RAMAN SPECTROSCOPIC STUDIES ON HUMAN-ENAMEL AND PRECIPITATED CARBONATE-CONTAINING APATITES. *Journal of Dental Research*, 1981, **60**(3), pp.751-755.
 96. KLEE, W.E. VIBRATIONAL SPECTRA OF PHOSPHATE IONS IN FLUORAPATITE. *Zeitschrift Fur Kristallographie Kristallgeometrie Kristallphysik Kristallchemie*, 1970, **131**(1-2), pp.95-&.
 97. LEVITT, S.R. and R.A. CONDRADE. VIBRATIONAL SPECTRA OF LEAD APATITES. *American Mineralogist*, 1970, **55**(9-10), pp.1562-&.
 98. ELLIOT, J. *Crystallographic structure of dental enamel and relative apatites* medicine thesis, the london hospital medical college 1961.
 99. STUTMAN, J.M. vibrational spectra and structure of phosphate ions in some calcium phosphates. *Trans. NY acad. Sci.*, 1965, **27**(6), pp.669-675.
 100. LEVITT, S.R.C., R. A. Vibrational spectra of lead apatites *American Mineralogist*, 1970, **49**(9-10), pp.1562-1575.
 101. BADDIEL, C.B.B., E E. . spectra-structure correlations in Hydroxyapatite and Fluorapatite *Spectrochimica Acta Part a-Molecular and Biomolecular Spectroscopy*, 1966, **22**(8), pp.1407-1416.